

Unconventional Quantum Sound-Matter Interactions in Spin-Optomechanical-Crystal Hybrid Systems

Xing-Liang Dong,¹ Peng-Bo Li,^{1,2,*} Tao Liu,^{2,3} and Franco Nori^{2,4}

¹MOE Key Laboratory for Nonequilibrium Synthesis and Modulation of Condensed Matter, Shaanxi Province Key Laboratory of Quantum Information and Quantum Optoelectronic Devices, School of Physics, Xi'an Jiaotong University, Xi'an 710049, China

²Theoretical Quantum Physics Laboratory, RIKEN Cluster for Pioneering Research, Wako-shi, Saitama 351-0198, Japan

³School of Physics and Optoelectronics, South China University of Technology, Guangzhou 510640, China

⁴Department of Physics, The University of Michigan, Ann Arbor, Michigan 48109-1040, USA



(Received 8 December 2020; accepted 16 April 2021; published 21 May 2021)

We predict a set of unusual quantum acoustic phenomena resulting from sound-matter interactions in a fully tunable solid-state platform in which an array of solid-state spins in diamond are coupled to quantized acoustic waves in a one-dimensional optomechanical crystal. We find that, by using a spatially varying laser drive that introduces a position-dependent phase in the optomechanical interaction, the mechanical band structure can be tuned *in situ*, consequently leading to unconventional quantum sound-matter interactions. We show that quasichiral sound-matter interactions can occur, with tunable ranges from bidirectional to quasiunidirectional, when the spins are resonant with the bands. When the solid-state spin frequency lies within the acoustic band gap, we demonstrate the emergence of an exotic polariton bound state that can mediate long-range tunable, odd-neighbor, and complex spin-spin interactions. This work expands the present exploration of quantum phononics and can have wide applications in quantum simulations and quantum information processing.

DOI: 10.1103/PhysRevLett.126.203601

Research of light-matter interactions in nanostructures injects new vitality into quantum optics [1]. The confinement of electromagnetic waves to small dimensions and engineered structures not only results in an enhanced light-matter coupling but also gives rise to new quantum phenomena such as chiral light-matter interactions [2–8], many-body physics in a band gap [9–13], and topological photonics [14–17]. These ideas are also explored in circuit quantum electrodynamics with superconducting qubits [18–21] and optomechanical systems [22–31].

Phonons, the quanta of mechanical waves, are potential candidates for implementing on-chip quantum information processing and networks because the speed of acoustic waves is much slower than that of light [32–36]. Moreover, mechanical systems can interface with various quantum emitters, ranging from superconducting circuits [37–40] and quantum dots [41] to solid-state defects [42–52]. In particular, hybrid systems composed of defect centers in diamond and phononic nanostructures (such as phononic waveguides or crystals) provide a promising platform for quantum applications due to their long coherent times and scalability [53–64]. However, compared to light, the realization of chiral sound-matter interactions remains an outstanding challenge due to the lack of polarization in phonons. Moreover, the rich physics resulting from quantum sound-matter interactions near acoustic band gaps remains largely unexplored.

In this work, we explore unconventional quantum interactions between sound and matter in a fully tunable solid-state device with silicon-vacancy (SiV) centers in diamond coupled to the acoustic waves in a 1D optomechanical crystal. We show that, through using optomechanical crystals [65–74], the acoustic band structures of sound waves can be tuned *in situ* by a suitably designed laser drive that introduces a position-dependent phase in the optomechanical interaction. Moreover, we find a number of unprecedented phenomena resulting from the interactions between solid-state spins and acoustic waves with tunable bands. When the spins are resonant with the bands, we predict a quasichiral sound-matter interaction with a tunable range from bidirectional to quasiunidirectional. When the spin frequency lies within the middle band gap, we analyze the emergence of an exotic bound state with alternating photon and phonon components. This polariton bound state can be exploited to mediate long-range tunable, odd-neighbor, and complex spin-spin interactions. The exclusive advantage of this highly tunable solid-state system is that the band structures of the acoustic waves and the resulting sound-matter interactions can be tuned *in situ*, thus providing a promising platform for the exploration of unusual quantum acoustic phenomena. This work opens new routes for quantum acoustics and could have applications in quantum simulations and quantum information processing, including the simulation of spin

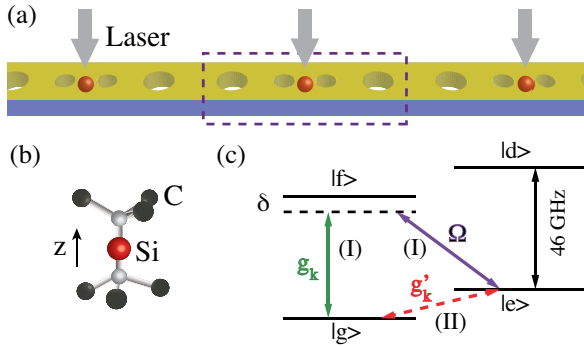


FIG. 1. (a) Schematic of a 1D optomechanical crystal embedded with SiV center arrays. The photons and phonons are colocalized in a nanocavity and two adjacent nanocavities are coupled via the tunneling effects or a waveguide. Physical structure (b) and coupling scheme of the electronic ground state (c) of a SiV center.

models [13], quantum state transfers [58,62], and entangled states preparation [75,76] via unidirectional phonon channels.

Model.—We consider a hybrid system of an array of SiV centers integrated to an optomechanical crystal, as depicted in Fig. 1. By deforming periodically the holes in an optomechanical crystal, an array of coupled defect cavities can form that strongly colocalizes phonons and photons. In each unit cell, there is a standard optomechanical interaction $\hat{H}_n = \hbar\omega_c \hat{a}_n^\dagger \hat{a}_n + \hbar\omega_M \hat{b}_n^\dagger \hat{b}_n - \hbar g_0 \hat{a}_n^\dagger \hat{a}_n (\hat{b}_n^\dagger + \hat{b}_n)$, where \hat{a}_n and \hat{b}_n are annihilation operators for photonic and phononic modes, respectively. The frequency of optical (acoustic) cavities ω_c (ω_M) and the coupling strength g_0 are assumed to be identical for each unit cell. The optical cavities are driven by a laser with a site-dependent phase $e^{-in\theta}$, which can be used to break the time-reversal symmetry, with $\theta \in [0, 2\pi]$ as a tunable constant. We derive the linearized interaction by replacing the cavity field $\hat{a}_n \rightarrow \hat{a}_n + \alpha e^{-in\theta} e^{-i\omega_L t}$ and keeping the terms up to first order in α , with α the average light-field amplitude of the laser and ω_L the driving frequency. For the intercell interaction, we assume the tight-binding model involving only the nearest-neighbor hoppings. We have verified the validity of this basic model via a full-wave simulation of the optomechanical system [77]. Thus, the whole Hamiltonian of the 1D optomechanical system in real space is given by ($\hbar = 1$)

$$\hat{H}_{OM} = \Delta/2 \sum_n \hat{a}_n^\dagger \hat{a}_n + \omega_M/2 \sum_n \hat{b}_n^\dagger \hat{b}_n - G \sum_n e^{-in\theta} \hat{a}_n^\dagger \hat{b}_n - J \sum_n \hat{a}_{n+1}^\dagger \hat{a}_n - K \sum_n \hat{b}_{n+1}^\dagger \hat{b}_n + H.c., \quad (1)$$

with detuning $\Delta = \omega_c - \omega_L$, enhanced coupling strength $G = g_0 \alpha$, and hopping rate J (K) for photons (phonons).

By imposing periodic boundary conditions and introducing the Fourier transformation $\hat{a}_k / \hat{b}_k = 1 / \sqrt{N} \sum_{n=1}^N e^{-iknd_0} \hat{a}_n / \hat{b}_n$ (d_0 is the lattice constant, and hereafter we choose $d_0 = 1$ for

simplicity), the optomechanical Hamiltonian in reciprocal space can be written as $\hat{H}_{OM} = \sum_k \hat{V}_k^\dagger \hat{H}(k) \hat{V}_k$, with $\hat{V}_k^\dagger = (\hat{a}_{k-\theta}^\dagger, \hat{b}_k^\dagger)$ and

$$\hat{H}(k) = \begin{bmatrix} -2J(k) & -G \\ -G & -2K(k) \end{bmatrix}. \quad (2)$$

Here, $J(k) = J \cos(k - \theta)$, $K(k) = K \cos(k)$, and $\Delta \approx \omega_M$ is taken as the energy reference. Physically, a phonon with momentum k is coupled to a photon with momentum $(k - \theta)$, resulting in asymmetric hybridization polaritons, when $\theta \neq \{0, \pi\}$. This Hamiltonian can be easily diagonalized as $\hat{H}_{OM} = \sum_k [\omega_u(k) \hat{u}_k^\dagger \hat{u}_k + \omega_l(k) \hat{l}_k^\dagger \hat{l}_k]$, where the polariton operators \hat{u}_k and \hat{l}_k are related to $\hat{a}_{k-\theta}$ and \hat{b}_k by means of a unitary transformation:

$$\begin{pmatrix} \hat{u}_k \\ \hat{l}_k \end{pmatrix} = \begin{pmatrix} -\sin \theta_k & \cos \theta_k \\ \cos \theta_k & \sin \theta_k \end{pmatrix} \begin{pmatrix} \hat{a}_{k-\theta} \\ \hat{b}_k \end{pmatrix}, \quad (3)$$

with $\sin \theta_k = -G / \sqrt{G^2 + [\omega_l(k) + 2K(k)]^2}$, $\cos \theta_k = -G / \sqrt{G^2 + [\omega_u(k) + 2K(k)]^2}$, and the dispersion

$$\omega_{u/l}(k) = -J(k) - K(k) \pm \sqrt{[K(k) - J(k)]^2 + G^2}. \quad (4)$$

The dispersion of polaritonic energy bands can be tuned and becomes either symmetric or asymmetric via changing θ , as shown in Figs. 2(a)–2(c). The bands are mostly optical and mechanical in nature except around the band edges (coupling points). Moreover, a sizable band gap ϵ_2 emerges and

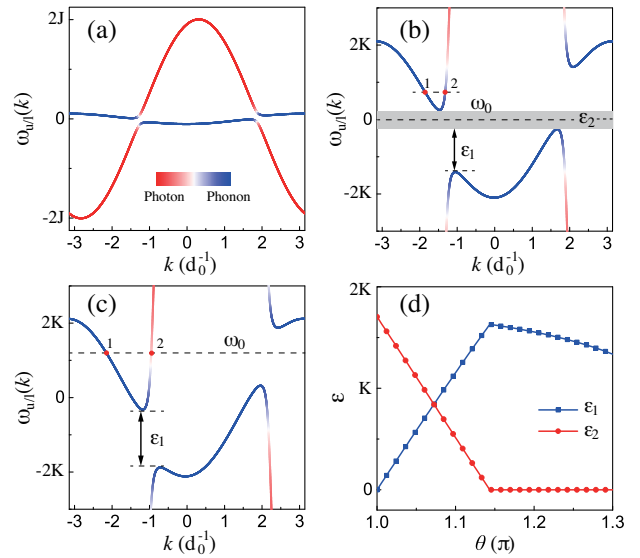


FIG. 2. Band structure $\omega(k)$ of a 1D optomechanical crystal under different system parameters. (a),(b) $\theta = 1.1\pi$. (c) $\theta = 1.2\pi$. (d) The size of band gap ϵ_2 and asymmetric area ϵ_1 as a function of θ . Here, $J = 20K$ and $G = 2K$. Note the relevant frequencies are shifted by $\Delta \approx \omega_M$.

can be tuned in a wide range of θ [see Figs. 2(b) and 2(d)]. In addition, the band asymmetry characterized by ε_1 is also tunable [see Figs. 2(b)–2(d)]. The band gap is maximized for $\theta = \pi$ and vanishes for $\theta \sim 1.14\pi$, where ε_1 reaches its maximum.

We now consider integrating a single or multiple solid-state spins into this 1D optomechanical crystal. In this work, we take into account SiV centers, as shown in Figs. 1(b) and 1(c). The levels $|g\rangle$ and $|e\rangle$ are coupled to the acoustic modes either (i) indirectly by a Raman process or (ii) directly by adding an off-axis magnetic field [50,58]. Thus, in terms of spin operators $\{\hat{\sigma}_z, \hat{\sigma}_+, \hat{\sigma}_-\}$, the free Hamiltonian is $\hat{H}_{\text{free}} = \omega_0/2 \sum_m \hat{\sigma}_z^m$, and the effective interaction Hamiltonian reads $\hat{H}_{\text{int}} = g_{\text{eff}} \sum_m (\hat{\sigma}_+^m \hat{b}_{x_m} + \text{H.c.})$. Here, ω_0 is the transition frequency of the effective two-level system, g_{eff} is the effective spin-phonon coupling strength, and x_m denotes the position at which the m th spin is coupled to the phononic waveguide. Lastly, working in momentum space, \hat{H}_{int} becomes

$$\hat{H}_{\text{int}} = \frac{g_{\text{eff}}}{\sqrt{N}} \sum_{k,m} \hat{\sigma}_+^m e^{ikx_m} (\cos \theta_k \hat{u}_k + \sin \theta_k \hat{l}_k) + \text{H.c.} \quad (5)$$

Band regime.—We consider the spins resonant with only the one side of upper band at the wave vector k_1 and k_2 in Figs. 2(b) and 2(c). The corresponding decay rates are $\gamma_1 = g_{\text{eff}}^2 \cos^2 \theta_{k_1} / |v_g^1|$ and $\gamma_2 = g_{\text{eff}}^2 \cos^2 \theta_{k_2} / |v_g^2|$, relating to the left ($v_g^1 < 0$) and right ($v_g^2 > 0$) propagating acoustic waves, with $\cos^2 \theta_{k_{1,2}}$ the weights of the phononic components of the polaritons in the upper band, and $v_g^{1,2} = \partial \omega / \partial k|_{\omega=\omega_0, k=k_{1,2}}$ the group velocity. The condition $\gamma_1 > \gamma_2$ is always maintained, which reflects the chiral coupling between the spins and the acoustic modes in the optomechanical crystal.

For the case of N SiV centers, the optomechanical-crystal-mediated interaction between the spins is realized by the emission and reabsorption of real polaritons propagating in the crystal, thus inheriting the chiral properties of the emission. However, in this system the exchange of virtual excitations between spins is possible, even in the dissipative regime, due to the interplay with the band edges on the other side of the Brillouin zone. Together with the band and band-edge-induced interactions, the spin dissipative dynamics is quasichiral. Unlike the unidirectional interaction exploiting helical topological edge states [86,87], here the quasichiral interaction results from the breakdown of the time-reversal symmetry in the topologically trivial acoustic band structure.

To gain more insight into this regime, we consider the Markovian approximation, where the degrees of freedom of the optomechanical crystal can be adiabatically eliminated. In this case, the effective motion equation describing the spin dynamics has the form $d\hat{\rho}_s/dt = \sum_{i,j} \Gamma_{ij} (\hat{\sigma}_-^i \hat{\rho}_s \hat{\sigma}_+^j - \hat{\sigma}_+^j \hat{\sigma}_-^i \hat{\rho}_s) + \text{H.c.}$ [88], where $\hat{\rho}_s$ is the reduced density

matrix for the spins, Γ_{ij} is the optomechanical-crystal-mediated interaction, $2\text{Re}(\Gamma_{ii}) = \gamma_1 + \gamma_2$ is the decay rate into the waveguide modes, and $\text{Im}(\Gamma_{ii})$ is the Lamb shift. In this system, the collective decay rates have the following expression [77]

$$\Gamma_{ij} = \lim_{s \rightarrow 0^+} \frac{g_{\text{eff}}^2}{2\pi} \int_{-\pi}^{\pi} dk e^{ikx_{ij}} \left\{ \frac{\cos^2 \theta_k}{s - i[\omega_0 - \omega_u(k)]} + \frac{\sin^2 \theta_k}{s - i[\omega_0 - \omega_l(k)]} \right\}, \quad (6)$$

with $x_{ij} = x_j - x_i$ the distance between two distant spins. We can divide Γ_{ij} into three parts as

$$\Gamma_{ij} = \text{P.V.}\Gamma_{ij} + \gamma_1 e^{ik_1 x_{ij}} \Theta(x_{ij}/v_g^1) + \gamma_2 e^{ik_2 x_{ij}} \Theta(x_{ij}/v_g^2),$$

with P.V. being the Cauchy's principal value, and Θ the Heaviside function defined such that $\Theta(0) = 1/2$. The second and third parts describe the dynamics dominated by the resonant k modes in which the polariton is emitted by spin i and then is recaptured by spin j , when $x_{ij} < 0$ (k_1 mode) and $x_{ij} > 0$ (k_2 mode), respectively. The probability of these two processes is different, i.e., $\gamma_1 \neq \gamma_2$, similar with chiral quantum optics [3,89,90]. In order to reveal the physics behind the Cauchy's principal value, we numerically plot $\text{P.V.}\Gamma_{ij}$ as a function of x_{ij} in Fig. 3(a). We find that it accounts for the long-range interaction induced by the band edges, with a strength $\max\{|g_{\text{edges}}^{ij}| \} < \gamma_1 \sim g_{\text{eff}}^2/2K$ and localized within $-15 \lesssim x_{ij} \lesssim 15$. Beyond this range, the coupling between the spin and the optomechanical crystal is completely chiral.

To gain insight into this chirality, we plot γ_2/γ_1 versus the spin frequency throughout the asymmetric area with different values of the phase gradient in Figs. 3(b) and 3(c). For $\theta = 1.1\pi$, we find $\gamma_2/\gamma_1 \rightarrow 1$ when ω_0 is close to the band edge. Away from the band edge, the ratio decreases very quickly. The chirality can be tuned from bidirectional to completely chiral. When $\theta = 1.2\pi$, we show that $\gamma_2/\gamma_1 \ll 1$ over the frequency range and in particular, we suggest a quasiunidirectional spin-phonon coupling when $\omega_0 \gtrsim 1.5K$, where $\gamma_2/\gamma_1 \lesssim 0.02$. Actually, for the quasiunidirectional channel in this case, $\sin^2 \theta_{k_1} < 0.01$ can be easily satisfied, such that the polariton is almost phononlike, which is more robust against the loss associated with optical decay.

Band-gap regime.—We now consider the situation where the middle band gap is opened and the spin frequency lies within this forbidden area for propagating photons and phonons. In this case, there exists an exotic bound state formed by single spins and polariton excitons in the single-excitation subspace. The bound state can be obtained by solving the secular equation $\hat{H}|\psi\rangle = E_{\text{BS}}|\psi\rangle$ [91,92], with $\hat{H} = \hat{H}_{\text{OM}} + \hat{H}_{\text{free}} + \hat{H}_{\text{int}}$, and the general form of the bound state

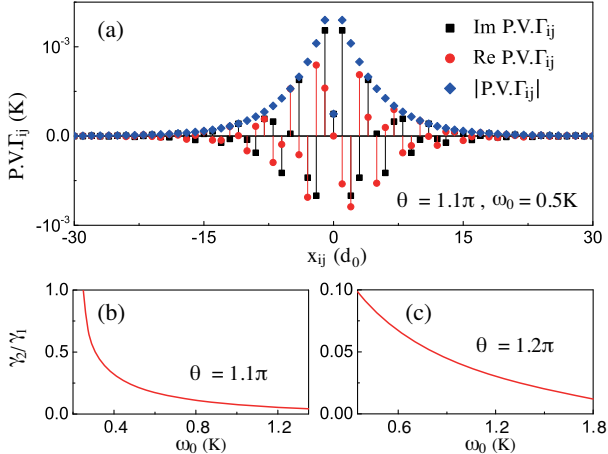


FIG. 3. (a) Cauchy's principal value of Γ_{ij} versus position x_{ij} with $\omega_0 = 0.5K$ and $\theta = 1.1\pi$. (b),(c) The ratio γ_2/γ_1 of decay into the right and left propagating modes of the crystal versus the spins frequency ω_0 .

$$|\psi\rangle = \left(C_e \hat{\sigma}_+ + \sum_{j=1}^N \sum_{\beta=a,b} C_{j,\beta} \hat{\beta}_j^\dagger \right) |g\rangle |\text{vac}\rangle, \quad (7)$$

where $|\text{vac}\rangle$ denotes the vacuum state of the 1D bath. The coefficients $|C_e|^2$, $|C_{j,a}|^2$, and $|C_{j,b}|^2$ are the probabilities for finding the excitations in the spin excited state and photonic and phononic bound states at the j th cell when the spin is coupled to the acoustic cavity at the $j = 0$ cell.

In Fig. 4, we plot the wave function distribution both in momentum and real space with $E_{\text{BS}} = 0$. First, we consider the symmetric case with the maximal value of the middle band gap ($\theta = \pi$). Figure 4(a) shows that the photon and phonon distributions in k space are symmetric ($k \rightarrow -k$), and more importantly, the conditions $C_{k,a} = C_{k+\pi,a}$ and $C_{k,b} = -C_{k+\pi,b}$ are satisfied, which is crucial to the enhancement and suppression of the wave function in certain neighbor sites in real space. In real space, we observe several features of the bound state, as shown in Figs. 4(b)–4(d). First, the bound state is localized in the vicinity of the spin with an exponential envelope, which is consistent with previous studies on band-gap-induced bound states in optical (acoustic) lattices [61,93]. The localization length is tunable when changing the system parameters such as the optomechanical coupling strength G .

The distinctive feature here is that the photon component only appears in the even cavities, while the phonon component only appears in the odd cavities, with respect to the cavity to which the spin is coupled. That is, the photon and phonon components of the bound state are staggered. Also the extra factors $(-1)^{j/2}$ and $(-1)^{(|j|-1)/2}$ determine the sign of $C_{a,j}$ and $C_{b,j}$. Moreover, the hybrid bound state obviously has a less photonic component, which makes this system more resilient to the dissipation

associated with photon decay. For the asymmetric case ($\theta = 1.1\pi$), the above features persist and another distinctive feature appears: the coefficients $C_{j,a}$ and $C_{j,b}$ are no longer real numbers but tunable complex numbers as a result of the asymmetric band structure, i.e., these describe a bound state with a tunable phase.

Now we consider the situation involving two or more SiV centers. When the band gap is much larger than the spin-phonon coupling strength (i.e., within the Markovian approximation), the effective spin interactions can be described as

$$\hat{H}_s = \sum_{i < j} (g_{ij} \hat{\sigma}_+^j \hat{\sigma}_-^i + g_{ij}^* \hat{\sigma}_+^i \hat{\sigma}_-^j), \quad (8)$$

which can be harnessed to simulate various quantum spin models [9,10]. Since spins are essentially coupled to phonon modes [94], the spin-spin coupling is only mediated by the phononic component of the bound state, with $g_{ij} = g_{\text{eff}} C_{j-i,b} / C_e$. From this expression, the spin-spin interactions can have a pattern similar to Fig. 4(d). The inheritance of the features from the bound state consequently leads to long-range tunable, odd-neighbor, and complex interactions between spins, which are still in the strong-coupling regime ($g_{ij} \gg \kappa_C \sum_j |C_{j,a}|^2$). This type of interaction is shown schematically in Fig. 4(e) with a short localization length involving only nearest-neighbor spins, and in Fig. 4(f) with a longer localization length involving far away odd-neighbor spins. To examine the validity of the

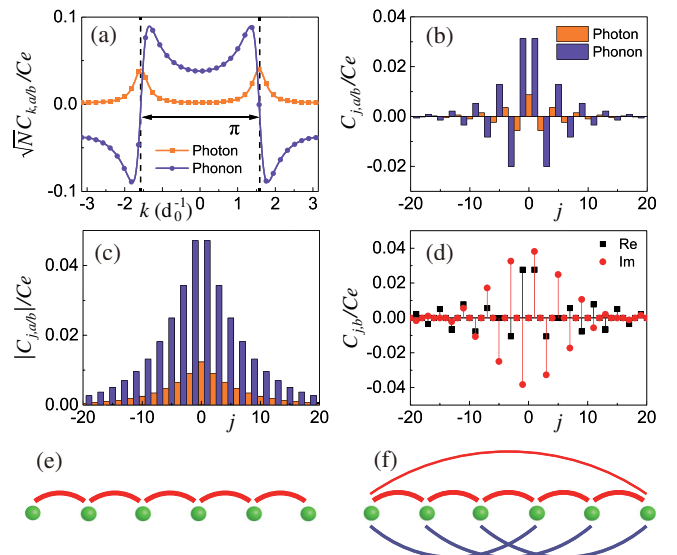


FIG. 4. (a),(b) Wave function distribution both in momentum $C_{k,a/b}$ and real space $C_{j,a/b}$ with $\theta = \pi$. (c) Modulus of the wave function distribution in real space $|C_{j,a/b}|$. (d) The real and imaginary parts of the wave function distribution for the acoustic phonons $\text{Re}(C_{j,b})$ and $\text{Im}(C_{j,b})$. $\theta = 1.1\pi$ in (c),(d). (e),(f) Long-range tunable, and odd-neighbor interactions in an array of spins with short (e) and long (f) localization length. Here, $g_{\text{eff}} = 0.08K$.

Markovian approximation for deriving the spin interactions in Eq. (8), we perform numerical simulations of the non-Markovian dynamics in the spin-optomechanical array system and find that the spin interactions can be well described by Eq. (8) (see Ref. [77] for details). Since the method for producing this type of spin-spin interaction is general, these spin interactions could be realized in other systems such as superconducting circuits [95–97] or photonic crystal platforms [98–100].

Experimental feasibility.—For actual implementations, we consider the 1D diamond optomechanical and photonic crystals with embedded individual color centers, as experimentally demonstrated in Refs. [69,71]. For the setups illustrated in Fig. 1, the diamond optomechanical crystal has mechanical frequencies about $2\pi \times 46$ GHz (or few GHz) and optical modes around $2\pi \times 200$ THz [68]. The programmable hopping rate for photons and phonons are $J \sim 20K$ and $K/2\pi \sim 50$ MHz, respectively [24,34,101,102]. In diamond nanostructures [68], the strong optomechanical coupling $G/2\pi \sim 100$ MHz is realizable [66]. Also, lasers with a position-dependent phase can be implemented on-chip by several methods [27,31,101,103]. With a high quality factor $Q \sim 10^7$, the optical and acoustic decay rates are $\kappa_C/2\pi \sim 20$ MHz and $\kappa_M/2\pi \sim 4.6$ kHz, leading to low waveguide losses in the high-cooperativity regime ($G^2/\kappa_C\kappa_M \gg 1$). By targeted ion implantation, SiV centers can be accurately implanted into the diamond crystal. At mK temperatures, the thermal excitations vanish and the intrinsic dephasing rate of the SiV centers is $\gamma_s/2\pi \sim 100$ Hz [57]. The strain-induced spin-phonon coupling strength can be calculated as $g_k/2\pi \sim 30$ MHz [58]. When choosing $\delta/2\pi \sim 450$ MHz and $\Omega/2\pi \sim 60$ MHz or an appropriate off-axis magnetic field [50], we have $g_{\text{eff}}/2\pi \sim 4$ MHz, $g_{12}/2\pi \sim 150$ kHz, and $\gamma_1/2\pi \sim 200$ kHz. In general, our system is still in the strong coupling regime.

Conclusion.—We have studied unconventional quantum sound-matter interactions in a tunable solid-state device with a combination of optomechanical crystals and SiV centers. We predict the emergence of quasichiral sound-matter interactions for the case of spins resonantly coupled to the band. We also show an exotic bound state with staggered photon and phonon components in the band-gap regime, which can be used to mediate long-range tunable, odd-neighbor, and complex spin-spin interactions. The work may be extended to higher dimensions or to other solid-state setups such as superconducting circuits.

We gratefully acknowledge the use of the open source Python numerical packages QUTIP [104,105]. P. B. L. is supported by the National Natural Science Foundation of China under Grants No. 92065105 and No. 11774285 and Natural Science Basic Research Program of Shaanxi (Program No. 2020JC-02). F. N. is supported in part by Nippon Telegraph and Telephone Corporation (NTT) Research, the Japan Science and Technology Agency

(JST) [via the Quantum Leap Flagship Program (Q-LEAP) program], the Moonshot R&D Grant No. JPMJMS2061, and the Centers of Research Excellence in Science and Technology (CREST) Grant No. JPMJCR1676], the Japan Society for the Promotion of Science (JSPS) [via the Grants-in-Aid for Scientific Research (KAKENHI) Grant No. JP20H00134 and the JSPS-RFBR Grant No. JPJSBP120194828], the Army Research Office (ARO) (Grant No. W911NF-18-1-0358), the Asian Office of Aerospace Research and Development (AOARD) (via Grant No. FA2386-20-1-4069), and the Foundational Questions Institute Fund (FQXi) via Grant No. FQXi-IAF19-06.

*Corresponding author.

lipengbo@mail.xjtu.edu.cn

- [1] D. E. Chang, J. S. Douglas, A. González-Tudela, C.-L. Hung, and H. J. Kimble, Colloquium: Quantum matter built from nanoscopic lattices of atoms and photons, *Rev. Mod. Phys.* **90**, 031002 (2018).
- [2] R. Mitsch, C. Sayrin, B. Albrecht, P. Schneeweiss, and A. Rauschenbeutel, Quantum state-controlled directional spontaneous emission of photons into a nanophotonic waveguide, *Nat. Commun.* **5**, 5713 (2014).
- [3] T. Ramos, H. Pichler, A. J. Daley, and P. Zoller, Quantum Spin Dimers from Chiral Dissipation in Cold-Atom Chains, *Phys. Rev. Lett.* **113**, 237203 (2014).
- [4] K. Y. Bliokh, D. Smirnova, and F. Nori, Quantum spin Hall effect of light, *Science* **348**, 1448 (2015).
- [5] K. Y. Bliokh, F.J. Rodríguez-Fortuño, F. Nori, and A. V. Zayats, Spin-orbit interactions of light, *Nat. Photonics* **9**, 796 (2015).
- [6] P. Lodahl, S. Mahmoodian, S. Stobbe, A. Rauschenbeutel, P. Schneeweiss, J. Volz, H. Pichler, and P. Zoller, Chiral quantum optics, *Nature (London)* **541**, 473 (2017).
- [7] C. Triolo, A. Cacciola, S. Patanè, R. Saija, S. Savasta, and F. Nori, Spin-momentum locking in the near field of metal nanoparticles, *ACS Photonics* **4**, 2242 (2017).
- [8] E. Sánchez-Burillo, C. Wan, D. Zueco, and A. González-Tudela, Chiral quantum optics in photonic sawtooth lattices, *Phys. Rev. Research* **2**, 023003 (2020).
- [9] A. González-Tudela, C.-L. Hung, D. E. Chang, J. I. Cirac, and H. J. Kimble, Subwavelength vacuum lattices and atom-atom interactions in two-dimensional photonic crystals, *Nat. Photonics* **9**, 320 (2015).
- [10] J. S. Douglas, H. Habibian, C.-L. Hung, A. V. Gorshkov, H. J. Kimble, and D. E. Chang, Quantum many-body models with cold atoms coupled to photonic crystals, *Nat. Photonics* **9**, 326 (2015).
- [11] J. D. Hood, A. Goban, A. Asenjo-Garcia, M. Lu, S.-P. Yu, D. E. Chang, and H. J. Kimble, Atom-atom interactions around the band edge of a photonic crystal waveguide, *Proc. Natl. Acad. Sci. U.S.A.* **113**, 10507 (2016).
- [12] A. González-Tudela and F. Galve, Anisotropic quantum emitter interactions in two-dimensional photonic-crystal baths, *ACS Photonics* **6**, 221 (2019).

- [13] M. Bello, G. Platero, J. I. Cirac, and A. González-Tudela, Unconventional quantum optics in topological waveguide QED, *Sci. Adv.* **5**, eaaw0297 (2019).
- [14] J. Perczel, J. Borregaard, D. E. Chang, H. Pichler, S. F. Yelin, P. Zoller, and M. D. Lukin, Topological Quantum Optics in Two-Dimensional Atomic Arrays, *Phys. Rev. Lett.* **119**, 023603 (2017).
- [15] K. Y. Bliokh, D. Leykam, M. Lein, and F. Nori, Topological non-hermitian origin of surface Maxwell waves, *Nat. Commun.* **10**, 580 (2019).
- [16] T. Ozawa, H. M. Price, A. Amo, N. Goldman, M. Hafezi, L. Lu, M. C. Rechtsman, D. Schuster, J. Simon, O. Zilberberg, and I. Carusotto, Topological photonics, *Rev. Mod. Phys.* **91**, 015006 (2019).
- [17] J. Perczel, J. Borregaard, D. E. Chang, S. F. Yelin, and M. D. Lukin, Topological Quantum Optics Using Atomlike Emitter Arrays Coupled to Photonic Crystals, *Phys. Rev. Lett.* **124**, 083603 (2020).
- [18] J. Q. You and F. Nori, Atomic physics and quantum optics using superconducting circuits, *Nature (London)* **474**, 589 (2011).
- [19] A. F. van Loo, A. Fedorov, K. Lalumi  re, B. C. Sanders, A. Blais, and A. Wallraff, Photon-mediated interactions between distant artificial atoms, *Science* **342**, 1494 (2013).
- [20] X. Gu, A. F. Kockum, A. Miranowicz, Y. xi Liu, and F. Nori, Microwave photonics with superconducting quantum circuits, *Phys. Rep.* **718–719**, 1 (2017).
- [21] W. Nie, Z. H. Peng, F. Nori, and Y.-x. Liu, Topologically Protected Quantum Coherence in a Superatom, *Phys. Rev. Lett.* **124**, 023603 (2020).
- [22] S. J. M. Habraken, K. Stannigel, M. D. Lukin, P. Zoller, and P. Rabl, Continuous mode cooling and phonon routers for phononic quantum networks, *New J. Phys.* **14**, 115004 (2012).
- [23] M. Aspelmeyer, T. J. Kippenberg, and F. Marquardt, Cavity optomechanics, *Rev. Mod. Phys.* **86**, 1391 (2014).
- [24] V. Peano, C. Brendel, M. Schmidt, and F. Marquardt, Topological Phases of Sound and Light, *Phys. Rev. X* **5**, 031011 (2015).
- [25] S. Kim, X. Xu, J. M. Taylor, and G. Bahl, Dynamically induced robust phonon transport and chiral cooling in an optomechanical system, *Nat. Commun.* **8**, 205 (2017).
- [26] E. Verhagen and A. Al  , Optomechanical nonreciprocity, *Nat. Phys.* **13**, 922 (2017).
- [27] A. Seif, W. DeGottardi, K. Esfarjani, and M. Hafezi, Thermal management and non-reciprocal control of phonon flow via optomechanics, *Nat. Commun.* **9**, 1207 (2018).
- [28] P. Rakich and F. Marquardt, Quantum theory of continuum optomechanics, *New J. Phys.* **20**, 045005 (2018).
- [29] H. Xu, L. Jiang, A. A. Clerk, and J. G. E. Harris, Nonreciprocal control and cooling of phonon modes in an optomechanical system, *Nature (London)* **568**, 65 (2019).
- [30] C. Sanavio, V. Peano, and A. Xuereb, Nonreciprocal topological phononics in optomechanical arrays, *Phys. Rev. B* **101**, 085108 (2020).
- [31] Z. Denis, A. Biella, I. Favero, and C. Ciuti, Permanent Directional Heat Currents in Lattices of Optomechanical Resonators, *Phys. Rev. Lett.* **124**, 083601 (2020).
- [32] M. V. Gustafsson, T. Aref, A. F. Kockum, M. K. Ekstr  m, G. Johansson, and P. Delsing, Propagating phonons coupled to an artificial atom, *Science* **346**, 207 (2014).
- [33] M. J. A. Schuetz, E. M. Kessler, G. Giedke, L. M. K. Vandersypen, M. D. Lukin, and J. I. Cirac, Universal Quantum Transducers Based on Surface Acoustic Waves, *Phys. Rev. X* **5**, 031031 (2015).
- [34] M. C. Kuzyk and H. Wang, Scaling Phononic Quantum Networks of Solid-State Spins with Closed Mechanical Subsystems, *Phys. Rev. X* **8**, 041027 (2018).
- [35] A. Bienfait, K. J. Satzinger, Y. P. Zhong, H.-S. Chang, M.-H. Chou, C. R. Conner,   . Dumur, J. Grebel, G. A. Peairs, R. G. Povey, and A. N. Cleland, Phonon-mediated quantum state transfer and remote qubit entanglement, *Science* **364**, 368 (2019).
- [36] Q. Bin, X.-Y. L  , F. P. Laussy, F. Nori, and Y. Wu, N-Phonon Bundle Emission via the Stokes Process, *Phys. Rev. Lett.* **124**, 053601 (2020).
- [37] Z.-L. Xiang, S. Ashhab, J. Q. You, and F. Nori, Hybrid quantum circuits: Superconducting circuits interacting with other quantum systems, *Rev. Mod. Phys.* **85**, 623 (2013).
- [38] Y. Chu, P. Kharel, W. H. Renninger, L. D. Burkhardt, L. Frunzio, P. T. Rakich, and R. J. Schoelkopf, Quantum acoustics with superconducting qubits, *Science* **358**, 199 (2017).
- [39] R. Manenti, A. F. Kockum, A. Patterson, T. Behrle, J. Rahamim, G. Tancredi, F. Nori, and P. J. Leek, Circuit quantum acoustodynamics with surface acoustic waves, *Nat. Commun.* **8**, 975 (2017).
- [40] K. J. Satzinger, Y. P. Zhong, H.-S. Chang, G. A. Peairs, A. Bienfait, M.-H. Chou, A. Y. Cleland, C. R. Conner,   . Dumur, J. Grebel, I. Gutierrez, B. H. November, R. G. Povey, S. J. Whiteley, D. D. Awschalom, D. I. Schuster, and A. N. Cleland, Quantum control of surface acoustic-wave phonons, *Nature (London)* **563**, 661 (2018).
- [41] M. Metcalfe, S. M. Carr, A. Muller, G. S. Solomon, and J. Lawall, Resolved Sideband Emission of InAs/GaAs Quantum Dots Strained by Surface Acoustic Waves, *Phys. Rev. Lett.* **105**, 037401 (2010).
- [42] S. Kolkowitz, A. C. Bleszynski Jayich, Q. P. Unterreithmeier, S. D. Bennett, P. Rabl, J. G. E. Harris, and M. D. Lukin, Coherent sensing of a mechanical resonator with a single-spin qubit, *Science* **335**, 1603 (2012).
- [43] C. Hepp, T. M  ller, V. Waselowski, J. N. Becker, B. Pingault, H. Sternschulte, D. Steinm  ller-Nethl, A. Gali, J. R. Maze, M. Atat  re, and C. Becher, Electronic Structure of the Silicon Vacancy Color Center in Diamond, *Phys. Rev. Lett.* **112**, 036405 (2014).
- [44] P.-B. Li, Y.-C. Liu, S.-Y. Gao, Z.-L. Xiang, P. Rabl, Y.-F. Xiao, and F.-L. Li, Hybrid Quantum Device Based on NV Centers in Diamond Nanomechanical Resonators Plus Superconducting Waveguide Cavities, *Phys. Rev. Applied* **4**, 044003 (2015).
- [45] D. A. Golter, T. Oo, M. Amezcuia, K. A. Stewart, and H. Wang, Optomechanical Quantum Control of a Nitrogen-Vacancy Center in Diamond, *Phys. Rev. Lett.* **116**, 143602 (2016).
- [46] P.-B. Li, Z.-L. Xiang, P. Rabl, and F. Nori, Hybrid Quantum Device with Nitrogen-Vacancy Centers in

- Diamond Coupled to Carbon Nanotubes, *Phys. Rev. Lett.* **117**, 015502 (2016).
- [47] D. A. Golter, T. Oo, M. Amezcuia, I. Lekavicius, K. A. Stewart, and H. Wang, Coupling a Surface Acoustic Wave to an Electron Spin in Diamond via a Dark State, *Phys. Rev. X* **6**, 041060 (2016).
- [48] D. Lee, K. W. Lee, J. V. Cady, P. Ovartchaiyapong, and A. C. B. Jayich, Topical review: Spins and mechanics in diamond, *J. Opt.* **19**, 033001 (2017).
- [49] M. K. Bhaskar, D. D. Sukachev, A. Sipahigil, R. E. Evans, M. J. Burek, C. T. Nguyen, L. J. Rogers, P. Siyushev, M. H. Metsch, H. Park, F. Jelezko, M. Lončar, and M. D. Lukin, Quantum Nonlinear Optics with a Germanium-Vacancy Color Center in a Nanoscale Diamond Waveguide, *Phys. Rev. Lett.* **118**, 223603 (2017).
- [50] S. Meesala, Y.-I. Sohn, B. Pingault, L. Shao, H. A. Atikian, J. Holzgrafe, M. Gündoğan, C. Stavrakas, A. Sipahigil, C. Chia, R. Evans, M. J. Burek, M. Zhang, L. Wu, J. L. Pacheco, J. Abraham, E. Bielejec, M. D. Lukin, M. Atatüre, and M. Lončar, Strain engineering of the silicon-vacancy center in diamond, *Phys. Rev. B* **97**, 205444 (2018).
- [51] P.-B. Li and F. Nori, Hybrid Quantum System with Nitrogen-Vacancy Centers in Diamond Coupled to Surface-Phonon Polaritons in Piezomagnetic Superlattices, *Phys. Rev. Applied* **10**, 024011 (2018).
- [52] S. Maity, L. Shao, S. Bogdanović, S. Meesala, Y.-I. Sohn, N. Sinclair, B. Pingault, M. Chalupnik, C. Chia, L. Zheng, K. Lai, and M. Lončar, Coherent acoustic control of a single silicon vacancy spin in diamond, *Nat. Commun.* **11**, 193 (2020).
- [53] G. Balasubramanian, P. Neumann, D. Twitchen, M. Markham, R. Kolesov, N. Mizuuchi, J. Isoya, J. Achard, J. Beck, J. Tissler, V. Jacques, P. R. Hemmer, F. Jelezko, and J. Wrachtrup, Ultralong spin coherence time in isotopically engineered diamond, *Nat. Mater.* **8**, 383 (2009).
- [54] P. Rabl, S. J. Kolkowitz, F. H. L. Koppens, J. G. E. Harris, P. Zoller, and M. D. Lukin, A quantum spin transducer based on nanoelectromechanical resonator arrays, *Nat. Phys.* **6**, 602 (2010).
- [55] S. D. Bennett, N. Y. Yao, J. Otterbach, P. Zoller, P. Rabl, and M. D. Lukin, Phonon-Induced Spin-Spin Interactions in Diamond Nanostructures: Application to Spin Squeezing, *Phys. Rev. Lett.* **110**, 156402 (2013).
- [56] N. Bar-Gill, L. Pham, A. Jarmola, D. Budker, and R. Walsworth, Solid-state electronic spin coherence time approaching one second, *Nat. Commun.* **4**, 1743 (2013).
- [57] D. D. Sukachev, A. Sipahigil, C. T. Nguyen, M. K. Bhaskar, R. E. Evans, F. Jelezko, and M. D. Lukin, Silicon-Vacancy Spin Qubit in Diamond: A Quantum Memory Exceeding 10 ms with Single-Shot State Readout, *Phys. Rev. Lett.* **119**, 223602 (2017).
- [58] M.-A. Lemonde, S. Meesala, A. Sipahigil, M. J. A. Schuetz, M. D. Lukin, M. Loncar, and P. Rabl, Phonon Networks with Silicon-Vacancy Centers in Diamond Waveguides, *Phys. Rev. Lett.* **120**, 213603 (2018).
- [59] C. Sánchez Muñoz, A. Lara, J. Puebla, and F. Nori, Hybrid Systems for the Generation of Nonclassical Mechanical States via Quadratic Interactions, *Phys. Rev. Lett.* **121**, 123604 (2018).
- [60] P.-B. Li, Y. Zhou, W.-B. Gao, and F. Nori, Enhancing Spin-Phonon and Spin-Spin Interactions Using Linear Resources in a Hybrid Quantum System, *Phys. Rev. Lett.* **125**, 153602 (2020).
- [61] P.-B. Li, X.-X. Li, and F. Nori, Band-gap-engineered spin-phonon, and spin-spin interactions with defect centers in diamond coupled to phononic crystals, *arXiv:1901.04650*.
- [62] M.-A. Lemonde, V. Peano, P. Rabl, and D. G. Angelakis, Quantum state transfer via acoustic edge states in a 2D optomechanical array, *New J. Phys.* **21**, 113030 (2019).
- [63] X.-X. Li, B. Li, and P.-B. Li, Simulation of topological phases with color center arrays in phononic crystals, *Phys. Rev. Research* **2**, 013121 (2020).
- [64] Y.-F. Qiao, H.-Z. Li, X.-L. Dong, J.-Q. Chen, Y. Zhou, and P.-B. Li, Phononic-waveguide-assisted steady-state entanglement of silicon-vacancy centers, *Phys. Rev. A* **101**, 042313 (2020).
- [65] A. H. Safavi-Naeini, T. P. M. Alegre, J. Chan, M. Eichenfield, M. Winger, Q. Lin, J. T. Hill, D. E. Chang, and O. Painter, Electromagnetically induced transparency and slow light with optomechanics, *Nature (London)* **472**, 69 (2011).
- [66] A. H. Safavi-Naeini, J. T. Hill, S. Meenehan, J. Chan, S. Gröblacher, and O. Painter, Two-Dimensional Phononic-Photonic Band Gap Optomechanical Crystal Cavity, *Phys. Rev. Lett.* **112**, 153603 (2014).
- [67] B. Khanaliloo, H. Jayakumar, A. C. Hryciw, D. P. Lake, H. Kaviani, and P. E. Barclay, Single-Crystal Diamond Nano-beam Waveguide Optomechanics, *Phys. Rev. X* **5**, 041051 (2015).
- [68] M. J. Burek, J. D. Cohen, S. M. Meenehan, N. El-Sawah, C. Chia, T. Ruelle, S. Meesala, J. Rochman, H. A. Atikian, M. Markham, D. J. Twitchen, M. D. Lukin, O. Painter, and M. Lončar, Diamond optomechanical crystals, *Optica* **3**, 1404 (2016).
- [69] A. Sipahigil, R. E. Evans, D. D. Sukachev, M. J. Burek, J. Borregaard, M. K. Bhaskar, C. T. Nguyen, J. L. Pacheco, H. A. Atikian, C. Meuwly, R. M. Camacho, F. Jelezko, E. Bielejec, H. Park, M. Lončar, and M. D. Lukin, An integrated diamond nanophotonics platform for quantum-optical networks, *Science* **354**, 847 (2016).
- [70] M. J. Burek, C. Meuwly, R. E. Evans, M. K. Bhaskar, A. Sipahigil, S. Meesala, B. Machielse, D. D. Sukachev, C. T. Nguyen, J. L. Pacheco, E. Bielejec, M. D. Lukin, and M. Lončar, Fiber-Coupled Diamond Quantum Nanophotonic Interface, *Phys. Rev. Applied* **8**, 024026 (2017).
- [71] R. E. Evans, M. K. Bhaskar, D. D. Sukachev, C. T. Nguyen, A. Sipahigil, M. J. Burek, B. Machielse, G. H. Zhang, A. S. Zibrov, E. Bielejec, H. Park, M. Lončar, and M. D. Lukin, Photon-mediated interactions between quantum emitters in a diamond nanocavity, *Science* **362**, 662 (2018).
- [72] J. V. Cady, O. Michel, K. W. Lee, R. N. Patel, C. J. Sarabalis, A. H. Safavi-Naeini, and A. C. B. Jayich, Diamond optomechanical crystals with embedded nitrogen-vacancy centers, *Quantum Sci. Technol.* **4**, 024009 (2019).
- [73] G. Calajó, M. J. A. Schuetz, H. Pichler, M. D. Lukin, P. Schneeweiss, J. Volz, and P. Rabl, Quantum acousto-optic control of light-matter interactions in nanophotonic networks, *Phys. Rev. A* **99**, 053852 (2019).

- [74] C. T. Nguyen, D. D. Sukachev, M. K. Bhaskar, B. Machielse, D. S. Levonian, E. N. Knall, P. Stroganov, R. Riedinger, H. Park, M. Lončar, and M. D. Lukin, Quantum Network Nodes Based on Diamond Qubits with an Efficient Nanophotonic Interface, *Phys. Rev. Lett.* **123**, 183602 (2019).
- [75] P.-B. Li, S.-Y. Gao, H.-R. Li, S.-L. Ma, and F.-L. Li, Dissipative preparation of entangled states between two spatially separated nitrogen-vacancy centers, *Phys. Rev. A* **85**, 042306 (2012).
- [76] K. Stannigel, P. Rabl, and P. Zoller, Driven-dissipative preparation of entangled states in cascaded quantum-optical networks, *New J. Phys.* **14**, 063014 (2012).
- [77] See Supplemental Material, which includes Refs. [78–85], at <http://link.aps.org/supplemental/10.1103/PhysRevLett.126.203601> for more details.
- [78] J. Chan, A. H. Safavi-Naeini, J. T. Hill, S. Meenehan, and O. Painter, Optimized optomechanical crystal cavity with acoustic radiation shield, *Appl. Phys. Lett.* **101**, 081115 (2012).
- [79] G. S. MacCabe, H. Ren, J. Luo, J. D. Cohen, H. Zhou, A. Sipahigil, M. Mirhosseini, and O. Painter, Nano-acoustic resonator with ultralong phonon lifetime, *Science* **370**, 840 (2020).
- [80] M. Schmidt, V. Peano, and F. Marquardt, Optomechanical metamaterials: Dirac polaritons, gauge fields, and instabilities, [arXiv:1311.7095](https://arxiv.org/abs/1311.7095).
- [81] S. Sokolov, J. Lian, E. Yüce, S. Combrié, A. D. Rossi, and A. P. Mosk, Tuning out disorder-induced localization in nanophotonic cavity arrays, *Opt. Express* **25**, 4598 (2017).
- [82] M. Sumetsky and Y. Dulashko, Snap: Fabrication of long coupled microresonator chains with sub-Angstrom precision, *Opt. Express* **20**, 27896 (2012).
- [83] E. Sánchez-Burillo, D. Porras, and A. González-Tudela, Limits of photon-mediated interactions in one-dimensional photonic baths, *Phys. Rev. A* **102**, 013709 (2020).
- [84] C. Cohen-Tannoudji, J. Dupont-Roc, G. Grynberg, and P. Thickstun, *Atom-Photon Interactions: Basic Processes and Applications* (Wiley Online Library, 1992).
- [85] L. Leonforte, A. Carollo, and F. Ciccarello, Vacancy-Like Dressed States in Topological Waveguide QED, *Phys. Rev. Lett.* **126**, 063601 (2021).
- [86] S. Barik, A. Karasahin, C. Flower, T. Cai, H. Miyake, W. DeGottardi, M. Hafezi, and E. Waks, A topological quantum optics interface, *Science* **359**, 666 (2018).
- [87] M. J. Mehrabad, A. P. Foster, R. Dost, E. Clarke, P. K. Patil, A. M. Fox, M. S. Skolnick, and L. R. Wilson, Chiral topological photonics with an embedded quantum emitter, *Optica* **7**, 1690 (2020).
- [88] H.-P. Breuer and F. Petruccione, *The Theory of Open Quantum Systems* (Oxford University Press on Demand, New York, 2002).
- [89] H. Pichler, T. Ramos, A. J. Daley, and P. Zoller, Quantum optics of chiral spin networks, *Phys. Rev. A* **91**, 042116 (2015).
- [90] T. Ramos, B. Vermersch, P. Hauke, H. Pichler, and P. Zoller, Non-markovian dynamics in chiral quantum networks with spins and photons, *Phys. Rev. A* **93**, 062104 (2016).
- [91] L. Zhou, H. Dong, Y.-x. Liu, C. P. Sun, and F. Nori, Quantum supercavity with atomic mirrors, *Phys. Rev. A* **78**, 063827 (2008).
- [92] J.-Q. Liao, Z. R. Gong, L. Zhou, Y.-x. Liu, C. P. Sun, and F. Nori, Controlling the transport of single photons by tuning the frequency of either one or two cavities in an array of coupled cavities, *Phys. Rev. A* **81**, 042304 (2010).
- [93] G. Calajó, F. Ciccarello, D. Chang, and P. Rabl, Atom-field dressed states in slow-light waveguide QED, *Phys. Rev. A* **93**, 033833 (2016).
- [94] F. Nori, R. Merlin, S. Haas, A. W. Sandvik, and E. Dagotto, Magnetic Raman Scattering in Two-Dimensional Spin-1/2 Heisenberg Antiferromagnets: Spectral Shape Anomaly and Magnetostrictive Effects, *Phys. Rev. Lett.* **75**, 553 (1995).
- [95] B. Peropadre, D. Zueco, F. Wulschner, F. Deppe, A. Marx, R. Gross, and J. J. García-Ripoll, Tunable coupling engineering between superconducting resonators: From sidebands to effective gauge fields, *Phys. Rev. B* **87**, 134504 (2013).
- [96] P. Roushan *et al.*, Chiral ground-state currents of interacting photons in a synthetic magnetic field, *Nat. Phys.* **13**, 146 (2017).
- [97] M. Mirhosseini, E. Kim, V. S. Ferreira, M. Kalaei, A. Sipahigil, A. J. Keller, and O. Painter, Superconducting metamaterials for waveguide quantum electrodynamics, *Nat. Commun.* **9**, 3706 (2018).
- [98] K. Fang, Z. Yu, and S. Fan, Realizing effective magnetic field for photons by controlling the phase of dynamic modulation, *Nat. Photonics* **6**, 782 (2012).
- [99] A. Majumdar, A. Rundquist, M. Bajcsy, V. D. Dasika, S. R. Bank, and J. Vučković, Design and analysis of photonic crystal coupled cavity arrays for quantum simulation, *Phys. Rev. B* **86**, 195312 (2012).
- [100] P. Lodahl, S. Mahmoodian, and S. Stobbe, Interfacing single photons and single quantum dots with photonic nanostructures, *Rev. Mod. Phys.* **87**, 347 (2015).
- [101] K. Fang, J. Luo, A. Metelmann, M. H. Matheny, F. Marquardt, A. A. Clerk, and O. Painter, Generalized non-reciprocity in an optomechanical circuit via synthetic magnetism and reservoir engineering, *Nat. Phys.* **13**, 465 (2017).
- [102] M. Mirhosseini, A. Sipahigil, M. Kalaei, and O. Painter, Superconducting qubit to optical photon transduction, *Nature (London)* **588**, 599 (2020).
- [103] S. Mittal, S. Ganeshan, J. Fan, A. Vaezi, and M. Hafezi, Measurement of topological invariants in a 2D photonic system, *Nat. Photonics* **10**, 180 (2016).
- [104] J. Johansson, P. Nation, and F. Nori, Qutip: An open-source python framework for the dynamics of open quantum systems, *Comput. Phys. Commun.* **183**, 1760 (2012).
- [105] J. Johansson, P. Nation, and F. Nori, Qutip 2: A python framework for the dynamics of open quantum systems, *Comput. Phys. Commun.* **184**, 1234 (2013).